

LETTER TO THE EDITOR

Molecular Gas in NUClei of GALaxies (NUGA): VI. Detection of a molecular gas disk/torus via HCN in the Seyfert 2 galaxy NGC 6951?*

M. Krips¹, R. Neri², S. García-Burillo³, F. Combes⁴, E. Schinnerer⁵, A.J. Baker⁶, A. Eckart⁷, F. Boone⁵, L. Hunt⁸, S. Leon⁹, and L.J. Tacconi¹⁰

¹ Harvard-Smithsonian Center for Astrophysics, SMA project, 645 N A'ohoku Pl., Hilo, HI, 96720, USA; e-mail: mkrips@cfa.harvard.edu

² Institut de Radio Astronomie Millimétrique (IRAM), Saint Martin d'Hères, F-38406, France

³ Observatorio Astronómico Nacional (OAN) - Observatorio de Madrid, C/ Alfonso XII 3, 28014 Madrid, Spain

⁴ Observatoire de Paris, LERMA, 61 Av. de l'Observatoire, 75014 Paris, France

⁵ Max-Planck-Institut für Astronomie, Königstuhl 17, 69117 Heidelberg, Germany

⁶ Department of Physics and Astronomy, Rutgers, the State University of NJ, 136 Frelinghuysen Rd., Piscataway, NJ 08854-8019, USA

⁷ Universität zu Köln, I. Physikalisches Institut, Zùlpicher Str. 77, 50937 Köln, Germany

⁸ INAF-Istituto di Radioastronomia/Sezione Firenze Largo E. Fermi 5, 50125 Firenze, Italy

⁹ IRAM, Avenida Divina Pastora, 7, Núcleo Central, 18012 Granada, Spain

¹⁰ Max-Planck-Institut für extraterrestrische Physik, Postfach 1312, 85741 Garching, Germany

ABSTRACT

Context. Several studies of nearby active galaxies indicate significantly higher HCN-to-CO intensity ratios in AGN (e.g., NGC 1068) than in starburst (e.g., M82) environments. HCN enhancement can be caused by many different effects, such as higher gas densities and/or temperatures, UV/X-ray radiation, and non-collisional excitation. As active galaxies often exhibit intense circumnuclear star formation, high angular resolution/high sensitivity observations are of paramount importance to disentangling the influence of star formation from that of nuclear activity on the chemistry of the surrounding molecular gas. The tight relation of HCN enhancement and nuclear activity may qualify HCN as an ideal tracer of molecular gas close to the AGN, providing complementary and additional information to that gained via CO.

Aims. NGC 6951 houses nuclear and starburst activity, making it an ideal testbed in which to study the effects of different excitation conditions on the molecular gas. Previous lower angular resolution/sensitivity observations of HCN(1–0) carried out with the Nobeyama Millimeter array by Kohno et al. (1999a) led to the detection of the starburst ring but no central emission has been found. Our aim was to search for nuclear HCN emission and, if successful, for differences of the gas properties of the starburst ring and the nucleus.

Methods. We used the new A, B, C and D configurations of the IRAM PdBI array to observe HCN(1–0) in NGC 6951 at high angular resolution ($1'' \approx 96$ pc) and sensitivity.

Results. We detect very compact (≤ 50 pc) HCN emission in the nucleus of NGC 6951, supporting previous hints of nuclear gas structure. Our observations also reveal HCN emission in the starburst ring and resolve it into several peaks, leading to a higher coincidence between the HCN and CO distributions than previously reported by Kohno et al. (1999a).

Conclusions. We find a significantly higher HCN-to-CO intensity ratio (≥ 0.4) in the nucleus than in the starburst ring (0.02–0.05). As for NGC 1068, this might result from a higher HCN abundance in the centre due to an X-ray dominated gas chemistry, but a higher gas density/temperature or additional non-collisional excitation of HCN cannot be entirely ruled out, based on these observations. The compact HCN emission is associated with rotating gas in a circumnuclear disk/torus.

Key words. Galaxies: individual (NGC 6951) – Galaxies: active – Galaxies: nuclei – Galaxies: Seyfert – Galaxies: starburst

1. Introduction

Over the past decade, several studies (e.g., Tacconi et al. 1994, Sternberg et al. 1994, Kohno et al. 1999a,b, 2000, 2001, 2005) have shown that the HCN-to-CO intensity ratio ($\equiv R_{\text{HCN/CO}}$) can be significantly higher in active galactic nuclei (AGN; e.g., NGC 1068) than in starburst (SB; e.g., M82) or quiescent re-

gions. While surprisingly large $R_{\text{HCN/CO}}$ (up to 1 or more) have been observed in AGN (e.g., NGC 1068, NGC 1097, NGC 5194; Kohno et al. 1999a, Tacconi et al. 1994, Usero et al. 2004), much smaller $R_{\text{HCN/CO}}$ (< 0.3) are detected in pure SB or composite (AGN+SB) galaxies (e.g., Arp220, M82, NGC 6951; Gao & Solomon 2004a,b, Nguyen-Q-Rieu et al. 1992). Inactive galaxies have even lower ratios of $R_{\text{HCN/CO}} < 0.1$. Many different effects can contribute to increased $R_{\text{HCN/CO}}$ in active environments including higher gas opacities/densities and/or temperatures, non-standard molecular abundances caused by strong UV/X-ray radiation fields or additional non-collisional excita-

Send offprint requests to: M. Krips

* Based on observations carried out with the IRAM Plateau de Bure Interferometer (PdBI). IRAM is supported by INSU/CNRS (France), MPG (Germany) and IGN (Spain).

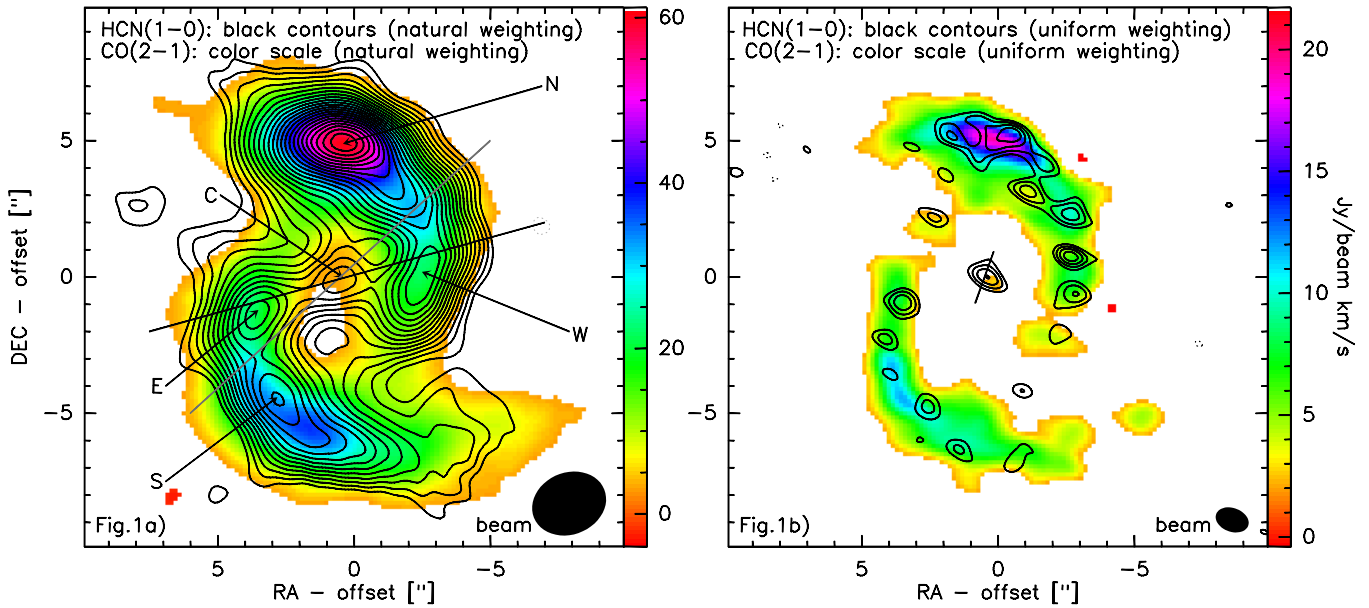


Fig. 1. Integrated HCN(1–0) emission (*black contours*) overlaid on CO(2–1) (*color scale*; Schinnerer et al., in prep., García-Burillo et al. 2005) in natural (*left*; 1a) and uniform weighting (*right*; 1b); the CO and HCN emission have been both integrated from -200 km s^{-1} to $+200\text{ km s}^{-1}$. We used a uv-taper for CO to match the angular resolution of our HCN data which is by a factor of ~ 2 lower, and obtain identical beamsizes. Black contours run from 3σ to 23σ (*right*: 7σ) in steps of $1\sigma=0.06\text{ Jy beam}^{-1}\text{ km s}^{-1}$ (*right*: $1\sigma=0.10\text{ Jy beam}^{-1}\text{ km s}^{-1}$); CO(2–1): $3\sigma=1.0\text{ Jy beam}^{-1}\text{ km s}^{-1}$ (*right*: $3\sigma=1.3\text{ Jy beam}^{-1}\text{ km s}^{-1}$). The black line (*left*) indicates the major axis of the bar (PA= 100°) and the grey line the major axis of the galaxy (PA= 130°). The black line (*right*) represents the most extreme central velocity gradients (PA=($160\pm 20^\circ$)). The (0,0) position is at $\alpha_{J2000}=20^{\text{h}}37^{\text{m}}14.123^{\text{s}}$ and $\delta_{J2000}=66^\circ06'20.09''$ which is slightly different from the phase centre of the observations.

tion such as IR pumping through UV/X-ray heated dust. Gao & Solomon (2004a) have ruled out the latter scenario for large scale HCN emission and the lack of any clear correlation between the hard X-ray and MIR luminosity in AGN (Lutz et al. 2004) reduces the significances of IR pumping also at small scales. However, Usero et al. (2004) present strong evidence in the case of NGC 1068 that the nuclear gas chemistry is dominated by X-ray radiation from the AGN yielding significantly different molecular abundances than in SB or quiescent environments (Lepp & Dalgarno 1996; Maloney et al. 1996). Recent IRAM 30m observations of several HCN transitions in a sample of 12 nearby active galaxies also seem to support a significantly higher HCN abundance in AGN than in SB or inactive environments, rather than a pure density/temperature or non-collisional excitation effect (Krips et al., in prep.). If true, this has a severe impact on the interpretation of $R_{\text{HCN/CO}}$ as a measure of the dense to total molecular gas mass fraction in active galaxies (e.g., Gao & Solomon et al. 2004a,b) as discussed in Graciá-Carpio et al. (2006). The study of nearby active galaxies also reveals the limitations of $R_{\text{HCN/CO}}$ as a unique diagnostic in distant sources whose starburst and AGN components cannot be separated.

NGC 6951 is an active galaxy of Hubble type SAB(rs)bc at a distance of 24 Mpc (Tully 1988); its active nucleus is classified as a transition object between a LINER and a type 2 Seyfert (Pérez et al. 2000). In addition to its AGN, NGC6951 also exhibits a pronounced SB ring at a radius of $5''$ ($\approx 480\text{ pc}$) in H α (Marquez & Moles 1993, Wozniak et al. 1995, Rozas et al. 1996; Gonzalez-Delgado & Perez 1997, Perez et al. 2000) and radio emission (Vila et al. 1990, Saikia et al. 1994 & 2002). Strong CO and HCN emission is associated with the SB ring (e.g., Kohno et al. 1999a, García-Burillo et al. 2005) while almost no emission had been hitherto found in the centre of NGC 6951. Only

Component	peak flux (mJy beam $^{-1}$)	FWHM (km s $^{-1}$)	$I_{\text{HCN}(1-0)}$ (Jy beam $^{-1}\text{ km s}^{-1}$)	$I_{\text{CO}(2-1)}^a$ (Jy beam $^{-1}\text{ km s}^{-1}$)
N	11 ± 2.0	150 ± 6	1.8 ± 0.2	60 ± 6
W	10 ± 1.0	100 ± 8	1.1 ± 0.1	22 ± 2
E	12 ± 1.0	70 ± 5	1.0 ± 0.1	23 ± 2
S	13 ± 1.0	60 ± 4	0.9 ± 0.1	38 ± 4
C b	4.8 ± 0.5	170 ± 20	0.9 ± 0.1	2.4 ± 0.2
Total flux c	36.0 ± 4.0^d	320 ± 14	12.0 ± 1.0^e	470 ± 50^e

Table 1. HCN(1–0) line parameters, obtained at the various peak (i.e., not spatially integrated) by fitting a Gaussian profile to the (naturally weighted) data. Errors include uncertainties of the fit and calibration. a from Schinnerer et al., in prep. b from uniformly weighted maps to avoid contamination by the ring emission. c spatially integrated over the entire area of $\pm 9''$; d in mJy; e in Jy km s $^{-1}$.

recently have high angular resolution/high sensitivity PdBI observations revealed faint CO(2–1) emission in the central $0.5''$ (García-Burillo et al. 2005; Schinnerer et al., in prep.). The latter observations are part of the PdBI NU(clei of)GA(laxies) project (e.g., García-Burillo et al. 2003). We observed NGC 6951 in HCN(1–0) to search for nuclear emission and assess differences between the SB ring and the AGN; the results of these observations are presented here.

2. Observations

NGC 6951 has been observed at 3mm and 1mm using all six antennae of the IRAM PdBI in the new A, B, C and D configurations (see <http://www.iram.fr> for telescope parameters) during January, February (A+B), April and May (C+D) 2006. The phase reference centre was set to $\alpha_{J2000}=20^{\text{h}}37^{\text{m}}14.470^{\text{s}}$

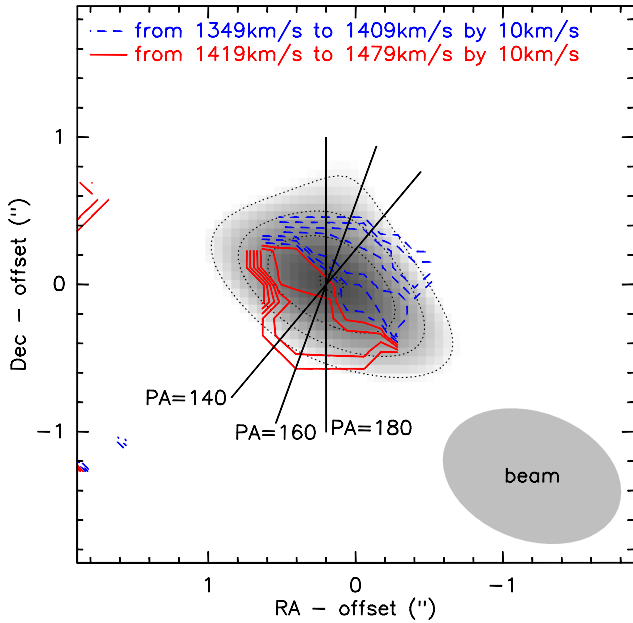


Fig. 2. Iso-velocity map of HCN(1–0) (solid red & dashed blue lines) overlaid to the integrated HCN(1–0) emission (grey scale & grey contours (same as in Fig. 1)). Contours run from $v_{\text{LSR}}=1349 \text{ km s}^{-1}$ (dashed blue) to 1479 km s^{-1} (solid red) in steps of 10 km s^{-1} around the dynamical center ($\sim 10 \text{ km s}^{-1}$ off from the systemic velocity). The black lines indicate the PA ($=160 \pm 20^\circ$) of the velocity gradient.

and $\delta_{J2000} = 66^\circ 06' 19.70''$. The 3mm receivers were tuned to the frequency of HCN(1–0) shifted to the LSR velocity of $v_{\text{LSR}} = 1424 \text{ km s}^{-1}$, while the 1mm receivers were set to the $^{13}\text{CO}(2-1)$ line. The 1mm data will be discussed in a separate paper (Krips et al., in prep.). Upper and lower sidebands at each frequency had 580 MHz bandwidth and 1.25 MHz resolution. Weather conditions were good throughout the observations with a water column varying between 4mm and 10mm and SSB system temperatures of 100–150 K (A+B) and 100–200 K (C+D) at 3mm. 3C273, 3C454.3, 2200+420 and 1749+096 were used as bandpass calibrators while 1928+738 and 2037+511 were used as gain calibrators. Fluxes have been calibrated with MWC349 and checked on 3C273, 1928+738 and 2037+511 with the flux monitoring program of the IRAM PdBI, resulting in an accuracy of $\sim 10\%$ at 3mm. The data were calibrated, mapped and analyzed using the standard IRAM GILDAS programs CLIC and MAPPING. Using uniform weighting, the synthesized beam size is $1.25'' \times 0.87''$ at a position angle (PA) of 72° at 3mm; natural weighting results in $2.78'' \times 2.27''$ at a PA of 112° . We reach an rms noise of $\sim 0.8 \text{ mJy beam}^{-1}$ ($\sim 1.2 \text{ mJy beam}^{-1}$) at a spectral resolution of 5 MHz ($\equiv 17 \text{ km s}^{-1}$) at 3.4 mm for natural (uniform) weighting.

3. Results & Discussion

3.1. Starburst ring

HCN emission is clearly detected along the starburst ring, consistent with Kohno et al. (1999a). The total flux observed with the PdBI is lower by a factor of ~ 2 –3 than the flux obtained with the IRAM 30m telescope (Krips et al., in prep.), i.e., some of the HCN emission is resolved out by the PdBI. The two main maxima, which are seen in HCN by Kohno et al. (1999a) at an angular resolution of $\sim 4.5''$ and peak at different positions than

CO, split up into several sub-maxima (N,W,E,S; Fig. 1) at the higher angular resolution ($< 3''$) of the PdBI. The HCN peaks N and S are consistent in position with those in CO (Fig. 1; García-Burillo et al. 2005). Additional HCN peaks are found to the west (W) and east (E) (see Fig. 1). The W-to-N and E-to-S peak ratios are higher in HCN (~ 0.6 – 1.0) than in CO (~ 0.4 – 0.6 ; Table 1) explaining why the positions of the merged peaks in Kohno et al. (1999a) do not agree between HCN and CO. The HCN-to-CO ratios ($\equiv R_{\text{HCN/CO}} = I_{\text{HCN}(1-0)} / I_{\text{CO}(1-0)}$; with $I \equiv$ velocity integrated intensity) thus also differ between the S/N and W/E peaks. While $R_{\text{HCN/CO}}$ is found to be roughly ~ 0.03 at S and N (assuming $I_{\text{CO}(2-1)} / I_{\text{CO}(1-0)} = 1$; Table 1), we estimate $R_{\text{HCN/CO}} \approx 0.05$ at E and W. This might indicate a variation of the gas density/temperature along the ring. The HCN kinematics in the ring agree well with those seen in CO and are hence not further discussed in this letter.

3.2. Central emission

HCN(1–0) emission is detected in the central $\sim 1''$ ($\approx 100 \text{ pc}$; $\equiv \text{C}$) because of the higher sensitivity and angular resolution of our data compared to the one obtained by Kohno et al. (1999a), confirming previous hints found in CO(2–1) (García-Burillo et al. 2005; Schinnerer et al., in prep.). The nuclear HCN component C appears to be compact and unresolved in the PdBI beam. Assuming the “HCN conversion” factor of $X_{\text{HCN}} (= M_{\text{HCN}}(\text{H}_2) / L_{\text{HCN}}) = 20^{+30}_{-10} \text{ M}_\odot (\text{K km s}^{-1} \text{ pc}^2)^{-1}$ from Solomon et al. (1992), we find a central dense gas mass of $M_{\text{gas}} (= M(\text{H}_2 + \text{He})) \approx (2-10) \cdot 10^7 \text{ M}_\odot$ which is a factor of ~ 3 – 17 higher than the mass of $\sim 6 \cdot 10^6 \text{ M}_\odot$ derived from the CO(2–1) line (assuming $I_{\text{CO}(2-1)} / I_{\text{CO}(1-0)} = 1$ (Table 1; see also García-Burillo et al. 2005). This large discrepancy cannot be solely due to the large uncertainties of the conversion factors but might further indicate non-standard gas conditions in the AGN. The HCN-to-CO ratio of the velocity integrated line flux amounts to ≥ 0.4 (Table 1; $I_{\text{CO}(2-1)} / I_{\text{CO}(1-0)} = 1$). This is a factor of ~ 4 – 8 larger than in the starburst ring and the value of 0.09 for the nucleus published by Kohno et al. (1999a) indicating that the nuclear HCN is significantly enhanced in NGC 6951. Thus, unlike Kohno et al. (1999a), we conclude that the nuclear gas properties in NGC 6951 are *not* that different from those in the Seyfert galaxies NGC 1068 or M51, both of which have similarly high central HCN-to-CO ratios. The molecular gas chemistry in the AGN influenced regions of NGC 1068 and NGC 5194 is dominated by X-ray radiation (NGC 1068: e.g., Usero et al. 2004; M51: e.g., Matsushita et al. 1998) suggesting a similar scenario in NGC 6951. Thus, the central dense gas mass derived via HCN has to be considered an upper limit.

The central HCN emission shows the steepest velocity gradient at $\text{PA} \approx 160^\circ$ with a velocity range of $\pm 70 \text{ km s}^{-1}$ around the dynamical center over a radius of $\sim 0.5''$ (Fig. 2), eventually indicating a gas rotation in a circumnuclear disk or torus. Even if accounting for the uncertainties of the PA, estimated to be $\pm 20^\circ$, the central kinematic axis is significantly different from the major axis of the galaxy ($\text{PA} = 135^\circ$) and of the bar ($\text{PA} = 100^\circ$). This non-alignment might be caused by a different inclination of the central gas disk/torus than of the galaxy, or, alternatively, by non-circular velocities or a warp. However, the central velocity gradient allows us to give a crude estimate of the enclosed dynamical mass. Assuming a radius of $\sim 50 \text{ pc}$ and a velocity range of $\pm 70 \text{ km s}^{-1}$, we find $M_{\text{dyn}} = 5 \cdot 10^7 \cdot (\sin i)^{-2} \text{ M}_\odot$, with $i \equiv$ inclination of the disk. This is similar to the gas mass of 0.6 – $8 \cdot 10^7 \text{ M}_\odot$, suggesting that the disk is seen closer to face-on

than to edge-on. Assuming further the inclination of the galaxy ($\approx 40^\circ$; García-Burillo et al. 2005) as rough estimate for the one of the central gas disk, the enclosed dynamical mass increases to $\sim 2 \cdot 10^8 M_\odot$. This is of the order of the nuclear black hole mass of $\sim 2 \cdot 10^8 M_\odot$, estimated via the stellar velocity dispersion of the bulge ($\sigma_s = 232 \text{ km s}^{-1}$ from Ho & Ulvestad 2001; see also Gebhardt et al. 2000). However, within a radius of 50 pc, stars might still contribute a significant fraction to the dynamical mass as well pointing towards an even lower inclination of the nuclear disk than assumed.

4. Conclusions

We have presented high angular resolution/sensitivity observations of the HCN(1–0) emission in NGC 6951 in this letter which exploit the new ABCD configurations at the IRAM PdBI. The main results can be summarized as follows:

1. The two main HCN peaks in the ring seen by Kohno et al. (1999a) split up into several sub-maxima which coincide with those found in CO(2–1) by García-Burillo et al. (2005) and Schinnerer et al. (in prep.). However, the ratios of peaks within the ring differ between HCN and CO, probably indicating different gas densities/temperatures along the ring.
2. We clearly detect compact HCN(1–0) emission in the nucleus of NGC 6951 tracing a dense molecular gas mass in the range of $\sim 0.6\text{--}6 \times 10^7 M_\odot$. A position velocity cut taken along $\text{PA} = (160 \pm 20)^\circ$, coinciding neither with the galaxy nor the bar major axis, yields the steepest velocity gradient in the nucleus. The gradient and the compactness of this central HCN emission suggest that it might arise in a rotating circumnuclear gas disk or torus with a radius of $\lesssim 50$ pc.
3. In contrast to Kohno et al. (1999a), we find significantly different HCN-to-CO line ratios in the starburst ring and the nuclear emission. While the starburst ring shows typical $R_{\text{HCN/CO}} = 0.02\text{--}0.05$, HCN is significantly enhanced in the centre with $R_{\text{HCN/CO}} \geq 0.4$. Either the molecular gas in the nucleus is denser and/or hotter than in the starburst ring, increasing $R_{\text{HCN/CO}}$, or the gas chemistry in the nucleus of NGC 6951 is dominated by X-ray radiation from the AGN, producing a higher nuclear HCN abundance and thus a higher $R_{\text{HCN/CO}}$ similar to the center of NGC 1068.

References

- Blake, G.A.; Sutton, E. C.; Masson, C. R.; Phillips, T. G., 1987, *ApJ*, 315, 621
 Gallimore, J.F.; Baum, S.A.; O’Dea, C.P., 2004, *ApJ*, 613, 794
 Gao, Yu; Solomon, Philip M., 2004a, *ApJS*, 152, 63
 Gao, Yu; Solomon, Philip M., 2004b, *ApJ*, 606, 271
 García-Burillo, S.; Combes, F.; Hunt, L. K.; Boone, F.; Baker, A. J.; Tacconi, L. J.; Eckart, A.; Neri, R.; Leon, S.; Schinnerer, E.; Englmaier, P., 2003, *A&A*, 407, 485
 García-Burillo, S.; Combes, F.; Schinnerer, E.; Boone, F.; Hunt, L. K., 2005, *A&A*, 441, 1011
 Gebhardt, K.; Bender, R.; Bower, G., et al., 2000, *ApJ*, 539, 13
 González-Delgado R.M., & Pérez E., 1997, *ApJS* 108, 199
 Graciá-Carpio, J.; García-Burillo, S.; Planesas, P.; Colina, L., 2006, *ApJ*, 640, L135
 Helfer, Tamara T.; Blitz, Leo, 1997, *ApJ*, 478, 162
 Ho, L.C., & Ulvestad, J.S., 2001, *ApJS*, 133, 77
 Kohno, K.; Kawabe, R.; Vila-Vilaró, B., 1999, *ApJ*, 511, 157
 Kohno, K.; Kawabe, R.; Vila-Vilaró, B., The Physics and Chemistry of the Interstellar Medium, Proc. of the 3rd Cologne-Zermatt Symposium in Zermatt, Sep. 22–25, 1998, Eds.: V. Ossenkopf, J. Stutzki, and G. Winnewisser, GCA-Verlag Herdecke
 Kohno, K., Kawabe, R., Shibatsuka, T., Matsushita, S., Imaging at Radio through Submillimeter Wavelengths, ASP Conference Proceedings, Vol. 217, ed. by J.G. Mangum and S.J.E. Radford. ASP, p.364
 Kohno, K.; Matsushita, S.; Vila-Vilar, B.; Okumura, S. K.; Shibatsuka, T.; Okiura, M.; Ishizuki, S.; Kawabe, R., The Central Kiloparsec of Starbursts and AGN: The La Palma Connection, ASP Conference Proc. Vol. 249, ed. by J.H. Knapen, J.E. Beckman, I. Shlosman, and T.J. Mahoney. ASP, 2001, p. 672.
 Kohno, K., The evolution of starbursts: The 331st W. and E. Heraeus Seminar, AIP Conference Proceedings, 2005, Volume 783, p. 203
 Lepp, S.; Dalgarno, A., 1996, *A&A*, 306, 21
 Lutz, D.; Maiolino, R.; Spoon, H.W.W.; Moorwood, A.F.M., 2004, *A&A*, 418, 465L
 Maloney, P.R.; Hollenbach, D.J.; Tielens, A.G., 1996, *ApJ*, 466, 561
 Pérez, E.; Márquez, I.; Marrero, I.; Durret, F.; González Delgado, R. M.; Masegosa, J.; Maza, J.; Moles, M., 2000, *A&A*, 353, 893
 Márquez I., & Moles M., 1993, *AJ*, 105, 2090
 Matsushita, S.; Kohno, K.; Vila-Vilaro, B.; Tosaki, T.; Kawabe, R., 1998, *ApJ*, 495, 267
 Nguyen, Q.-R.; Jackson, J.M.; Henkel, Ch.; Truong, B.; Mauersberger, R., 1992, *ApJ*, 399, 521
 Rozas M., Beckman J.E., Knapen J.H., 1996, *A&A* 307, 735
 Saikia D.J., Pedlar A., Unger S.W., et al., 1994, *MNRAS*, 270, 46
 Saikia, D. J.; Phookun, B.; Pedlar, A.; Kohno, K., 2002, *A&A*, 383, 98
 Solomon, P.M.; Downes, D.; Radford, S.J.E., 1992, *ApJ*, 387, 55
 Sternberg, A.; Genzel, R.; Tacconi, L., 1994, *ApJ*, 436, 131
 Tacconi, L.J.; Genzel, R.; Blietz, M.; Cameron, M.; Harris, A.I.; Madden, S., 1994, *ApJ*, 426, 77
 Tacconi, L. J.; Blietz, M.; Cameron, M.; Downes, D.; Genzel, R.; Krabbe, A.; Sternberg, A.; Tacconi-Garman, L. E.; Weitzel, L., 1996, *VA*, 40, 23
 Tielens, A.G.G.M., & Hollenbach, D., 1985, *ApJ*, 291, 722
 Tully, R.B., 1988, *Nearby Galaxies Catalogue* (Cambridge University Press, Cambridge)
 Usero, A.; García-Burillo, S.; Fuente, A.; Martín-Pintado, J.; Rodríguez-Fernández, N. J., 2004, *A&A*, 419, 897
 Vila M.B., Pedlar A., Davies R.D., et al., 1990, *MNRAS* 242, 379
 Wozniak H., Friedli D., Martinet L., et al., 1995, *A&AS*, 111, 115